ACADEMIC PRESS

Available online at www.sciencedirect.com
SCIENCE DIRECT®

Journal of Catalysis 216 (2003) 144–154

JOURNAL OF CATALYSIS

www.elsevier.com/locate/jcat

Electron microscopy of catalysts: recent achievements and future prospects

Abhaya K. Datye

Department of Chemical and Nuclear Engineering and Center for Microengineered Materials, the University of New Mexico, Albuquerque, NM 87131, USA

Received 8 July 2002; revised 30 September 2002; accepted 22 October 2002

Abstract

Electron microscopy is undoubtedly one of the most important tools for visualizing the morphology of industrial heterogeneous catalysts. With improvements in resolution, it is now possible to directly image the complex nanostructure of catalytic materials. Spectroscopic measurements performed in situ within the microscope provide elemental analysis and information on oxidation state and bonding. The development of in situ, controlled atmosphere instruments means that we can now study working catalysts, instead of simply doing postmortem examinations. In this review, we assess the state of the art and highlight some of the insights provided by microscopy in the study of catalysts. We then look to the future to see the developments on the horizon (notably aberration-corrected microscopy) that could have the largest impact on our ability to understand catalysts.

Keywords: Electron microscopy; Model catalysis; Nanoparticle surfaces; Restructuring of catalysts; Sintering of catalysts; Scanning electron microscopy

1. Introduction

Since the invention of the transmission electron microscope, electron microscopy has been a key technique in allowing us to see the atomic scale structure of materials. Steady improvements in instrumental resolution and availability of in situ spectroscopies have only increased the importance of electron microscopy for the study of catalysts. Both scanning and transmission electron microscopes (SEMS/TEMS) are capable of providing information on the nanoscale structures seen in heterogeneous catalysts. In the past decade, the advent of scanning probe microscopes (STM/AFM) have provided images with even higher spatial resolution, and real time images of adsorbates in motion. However, these scanning probe techniques are best suited for the study of flat surfaces and of model catalysts. To gain insight into the three-dimensional structure of industrially relevant heterogeneous catalysts, electron microscopy remains a vital tool in the arsenal of the catalytic chemist.

The purpose of this review is to highlight the insights provided by electron microscopy for the study of heterogeneous catalysts, while assessing the state of the art in the application of electron microscopy today. In keeping with the spirit of this 40th anniversary special commemorative issue of the *Journal of Catalysis*, we start with a historical overview, attempting to put into perspective some of the achievements over the past two decades. Finally, we ask the question: what would heterogeneous catalysis want from an ideal electron microscope and which improvements are likely around the corner. This is not meant to be an exhaustive survey; the reader is directed to several recent reviews for further information [1–4].

2. Historical perspective

The electron microscope was developed by Ernst Ruska in 1939. He received a Nobel Prize for his contributions in 1986. We can gain a sense of electron microscopy during its infancy from the 1945 paper by Turkevich [5], one of the earliest surveys of the application of electron microscopy to the study of catalysts. The microscope used had a resolution limit of 50 Å; however, many of the problems described in this survey remain topics of intense study today. A common theme was the study of catalysts treated at high temperatures (600 °C in this case), leading to the disappearance of small Pt particles, and a loss of metal surface area. Another example reported by Turkevich [5] was the sintering of alumina, which lost surface area (from 270 to 13 m^2/g) after heating

E-mail address: datye@unm.edu.

0021-9517/03/$ – see front matter
doi:10.1016/S0021-9517(02)00113-6

at 600 °C. Since then, we have made significant improvements in our ability to stabilize metals and oxides, pushing up the temperature at which catalysts are stable. Recent studies of catalyst sintering for automotive and for combustion applications have been performed at temperatures of 900 °C [6] and 1300 °C [7], respectively.

The methods used to prepare catalyst samples for electron microscopy remain much the same as those used by Turkevich [5]. The sample is dispersed in a solvent to break up agglomerates, and a drop of the powder suspension is deposited on a carbon film that contains micrometer-sized and smaller holes. These "holey" carbon films allow us to image thin regions of solid samples without the elaborate sample preparation methods that are necessary for other classes of samples, such as metals, polymers, and ceramics [8]. In the application of microscopy to catalysts today, several other approaches are used. By dispersing the catalyst powder within an epoxy and using a microtome, we can prepare thin sections that provide better statistics and show the relative placement of various components within a catalyst [9]. It is even possible to study structures in solution that would otherwise be altered when the solvent is removed. Cryo TEM uses ultrafast cooling with liquid alkanes to freeze a sample without causing crystallization of the solvent. In this manner, organic and inorganic polymer structures can be preserved within amorphous ice for study in an electron microscope [10].

Major improvements in the resolution and spectroscopic capabilities of transmission electron microscopes have occurred in the past two decades. Notable among these are the development of high-voltage electron microscopes (200 keV and above) in Japan, UK, and the Netherlands that could resolve the atomic structure of ceramics and metals. Two numbers are typically reported for the resolution of a TEM, the point resolution (or the ability to directly interpret the observed image in terms of atomic structure) and the line resolution (or the information limit). The point resolution is limited not by the wavelength of the electrons, since the wavelength of 200 keV electrons is already 0.0251 Å. Rather, it is the spherical aberrations of the lenses, the stability of the microscope high voltage (chromatic aberration), and mechanical vibrations that limit the attainable resolution. The line resolution is affected by the stability of the microscope. In contrast, with scanning electron microscopes as well as scanning transmission microscopes (STEM), resolution is directly limited by the size of the electron probe.

Since the TEM image involves the passage of an electron wave through a three-dimensional sample, computational methods had to be developed to predict the effect of lens imperfections, instabilities, and the electron scattering within the sample. One of the earliest high-resolution images (better than 10-Å resolution) which could be directly interpreted in terms of the atomic structure of the material (a complex oxide) was reported by Iijima in 1971 [11]. The resolution of the microscope, a specially modified 100-keV microscope, was about 3.5 Å. Since then, improvements in electron optics have allowed the resolution of the most widely used 200-keV high-resolution TEMs to approach 1.8 Å. This means that the atomic structure of most metals and ceramics along their low index zone axes can be routinely resolved in modern TEMs. The race is now on to develop sub 1-Å resolution to allow study of atomic structures around defects, with the earliest reports of resolution at this scale being achieved by focal series restoration [12,13] or via holographic methods [14] that allow for correction of microscope aberrations.

3. Imaging of single atoms

For the application to heterogeneous catalysts, the more important question is the ability to resolve the smallest metal particles and clusters which are present on high-surface-area porous oxide supports. Often, it is the contrast from the support that limits our ability to detect the smallest structures. In 1971, Albert Crewe and his coworkers [15] showed that individual heavy atoms sitting on a light-atom supporting substrate could be imaged using dark field imaging in a scanning transmission electron microscope. In this case, the choice of a heavy atom (W) and a low contrast substrate (carbon film) was critical. Routine identification of single atoms of catalytically active metals such as Pt or Au on conventional silica or alumina supports is not yet possible. To achieve such imaging, the best approach would be to use high-angle annular dark field (HAADF) imaging which uses electrons scattered at high angles to form the image. Electron scattering at high angles is caused by scattering from the nucleus, Rutherford scattering, which follows a Z^2 dependence. Therefore, this form of imaging is also called Z-contrast imaging. A high brightness source of electrons, field emission gun (FEG), is necessary to create a fine probe which is scanned on the sample surface. The imaging is largely incoherent at these high angles; hence the image resolution is limited by the size of the probe. HAADF imaging could, until now, only be performed in dedicated STEM instruments making this technique less widely available. However, the advent of FEG combination TEM/STEM instruments is making this technique more widely available. At present, a resolution better than 2 Å is routinely available with these 200-keV instruments, and under ideal conditions a resolution of 1.4 Å is attainable [16].

The state of the art in HAADF imaging of small clusters is shown in Fig. 1 from the work of Pennycook [17] using a 1.4-Å probe in a 300-keV dedicated STEM instrument. The noise in the image from the support and from the finite probe size reduces the visibility of what are reported to be trimers of Pt on the alumina surface. Correction of aberrations in these instruments could reduce the probe size to below 1 Å leading to significant improvement in the ability to detect single atoms and small clusters. Fig. 2 shows a simulation of the image that could be obtained from the same sample using an aberration-corrected STEM instrument. Several such instruments are being constructed at present and it is

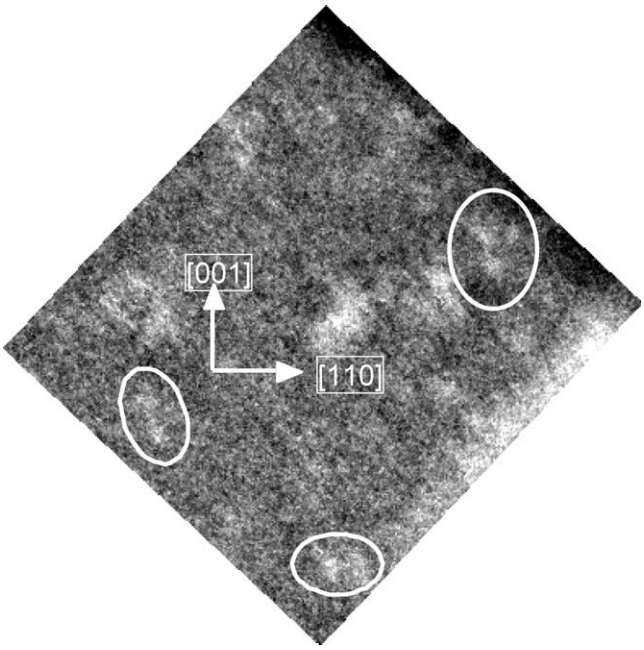

Fig. 1. Pt dimers and trimers imaged on a γ-alumina support using a 1.4-Å probe. The [001] and [110] directions of the spinel lattice are indicated. A smaller probe size (see simulated image in Fig. 2) would make it possible to see the Pt atoms clearly and also resolve the O atom columns (reprinted from [17] with the permission of the Microscopy Society of America).

hoped that these will revolutionize the study of single atoms and small clusters present on the surface of conventional oxide supports used in heterogeneous catalysts. It may be possible in the future to see all of the metal atoms that are deposited on the catalyst support.

4. Imaging of metal clusters (three atoms and larger)

While microscopists are still struggling to obtain images of single atoms, the picture is much better with regard to clusters containing three or more atoms. There are two major problems in accurately quantifying the size and distribution of small clusters. First, the phase contrast from the support makes detection of small clusters difficult. Second, the clusters may be present at different heights in the specimen. When the cluster is not exactly at the focal plane, it will appear more diffuse and the apparent size will be overstated. A rather pessimistic view was presented by Flynn et al. [18] in the 1970s, who predicted that size measurements from TEM images of particles smaller than 25 Å could be in significant error. Thankfully, improvements in the resolution of TEMs pushed down this uncertainty limit, to below 10 Å at present. For ease of imaging small clusters, a crystalline support imaged off its zone axis is preferable to amorphous supports such as carbon or silica. Such an approach was used by Schwank et al. [19] to image three-atom Os clusters on Al_2O_3, which were seen as scattering centers 6 Å in size. In more recent work, Allard et al. [20] have presented images of five-atom Os clusters, which appear as uniform black dots on the background of the support lattice (see Fig. 3). The 2.1-Å spacing of the MgO lattice planes provides an internal calibration to determine with high accuracy the size of these Os clusters. The problems of cluster visibility and changes in apparent size with focus still remain, but they can be overcome when dark field imaging in a STEM instrument is used.

In a STEM instrument, a fine electron probe is scanned over the sample to form the image. When electrons scattered at high angles are utilized with an annular detector, the technique is referred to as high-angle annular dark field imaging. HAADF images improve the visibility of small clusters since there is no phase contrast from the support. However, as seen in Fig. 1, the images are quite noisy and since the probe size is convoluted with that of the cluster, the apparent size will be overstated. To overcome this limitation, Treacy and coworkers at Exxon [21] measured the absolute intensity of scattered electrons, after the contribution from the nearby support was subtracted. Since scattered intensity is directly proportional to the number of atoms in the

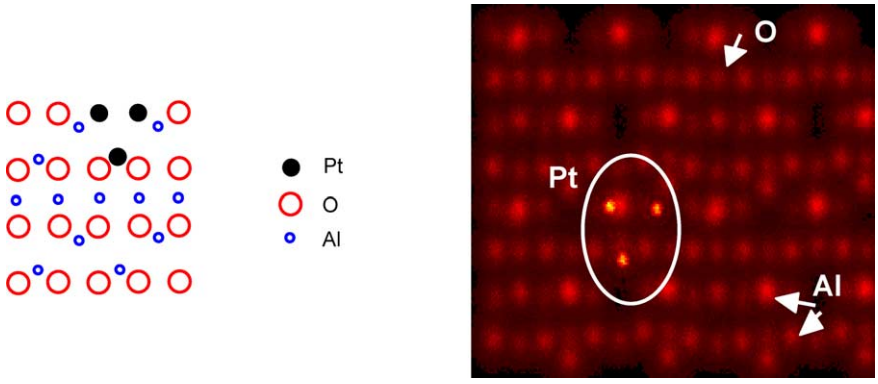

Fig. 2. (Left) surface monolayer of γ-alumina with Pt trimer in surface vacancy sites. (Right) simulated image of a Pt trimer on 50 Å of γ-alumina for the aberration-corrected VG HB603U microscope. Atom positions were obtained from first-principles simulations and the image simulated by convolution with the probe intensity profile. The simulation assumes a 0.5-Å probe for the surface atoms, but for the crystal the resolution will be limited by the size of the 1s Bloch states, approximately 0.8-Å diameter. The atomic positions of Pt atoms are directly visible as are oxygen columns in the support (reprinted from [17] with the permission of the Microscopy Society of America).

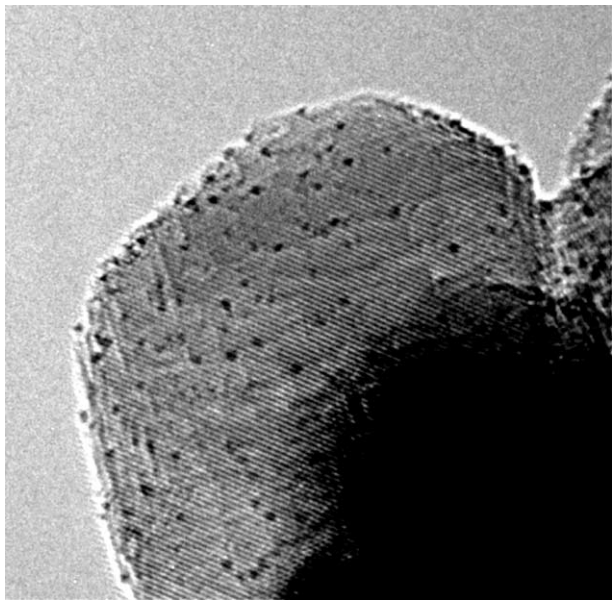

Fig. 3. High-resolution TEM image of $[Os_5C(CO)_{14}]^{2-}$ clusters on MgO. The MgO lattice fringe spacing of 2.1 Å serves as a calibration for the size of the clusters (reprinted from [20] with permission from American Chemical Society).

cluster, it provides a measure of the number of atoms. For a STEM probe size of 3.5 Å, Pt clusters containing as few as three atoms could be detected when supported on typical, 20-nm thick, γ-Al_2O_3 oxide support. In a subsequent study reported in 1990 [22], the Treacy group using a 2-Å probe demonstrated detection of single Pt atoms in a 200-Å thick zeolite support. The problem of probe convolution was recently addressed by Yang et al. [23], who studied the absolute intensity of Rutherford scattering as a function of measured particle diameter. The intensity scaled with diameter, but the variation was closer to d^4 than the expected d^3 relationship for spheres. Convolution of the cluster size with the finite probe impacted the apparent sizes of the smallest clusters much more than the larger clusters. By accounting for the probe size convolution effect, Yang et al. [23] were able to explain their d^4 scaling relationship and concluded that the clusters were spherical in shape throughout the size range investigated. This is in agreement with the previous work of Treacy et al. [21], who came to a similar conclusion.

5. Particle shapes and internal structures of small metal particles

As particles get larger than 20 Å, it becomes possible to discern their shapes and the nature of surface facets. The earliest images of the internal structure of small particles came from the Cambridge high-voltage microscope project through the work of Marks and Smith [24,25]. Their images, where the metal particles were imaged in profile view, provided the first glimpse of the internal structure of small metal

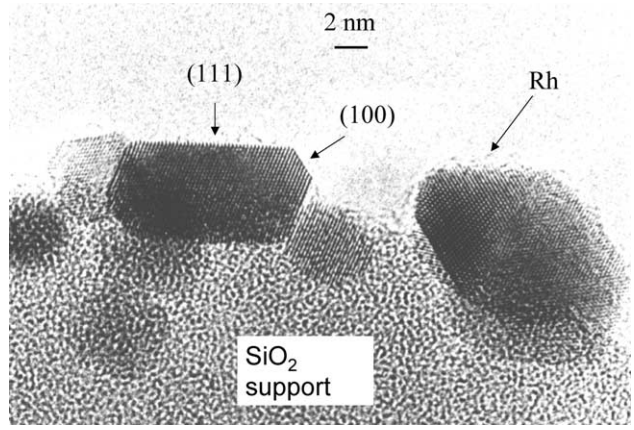

Fig. 4. Profile view images of Rh/SiO_2. Particles are nearly cubooctahedral and exhibit (111) and (100) facets (reprinted from [26] with permission from American Chemical Society).

particles relevant to catalysis. Fig. 4 shows a profile view image of a Rh metal particle on a model silica support prepared in our laboratory [26]. The silica microspheres make it easier to obtain profile views allowing us to clearly see the surfaces and metal-support interfaces in metal particles.

An important contribution over this period came from the group of Yacaman and Ocanaz [27], who developed the weak beam dark field technique to study the shape of small metal particles. The most common particle shape for fcc metals such as Pt or Au were cubooctahedral, as seen in Fig. 4 with particles exposing their (111) and (100) surface facets. While metal particles generally follow the atomic arrangements seen in the bulk metal, it was found that small particles irradiated by the electron beam can adopt a range of internal structures, with different arrangements such as bcc, hcp, or fcc, and even icosahedral observed on a given particle [28]. Nonetheless, the particles imaged in these studies were always three-dimensional, and no 2D or raftlike structures were reported. Around this time, workers at Exxon reported the observation of strong metal support interactions in the Pt/TiO_2 catalyst system. In situ TEM studies showed that Pt metal particles showed lower contrast after reduction in H_2, which was attributed to raftlike or pillbox structures [29]. However, later work using profile imaging confirmed that high-temperature reduction led to migration of a TiO_x overlayer rather than a change in the shape of metal particles [30].

There were other reports of raftlike structures, for example, the work by Yates et al. [31]. These reports were based on the contrast exhibited by the metal particles, dark particles being considered three-dimensional, whereas those exhibiting light contrast were thought to be rafts. This assertion was disputed by Treacy et al. [32], who demonstrated that contrast from metal particles depends on their diffraction condition, particles oriented correctly for diffraction appear dark, and no inference should therefore be made about three-dimensional shapes based on image contrast. The development of nonporous spherical model supports [33] by

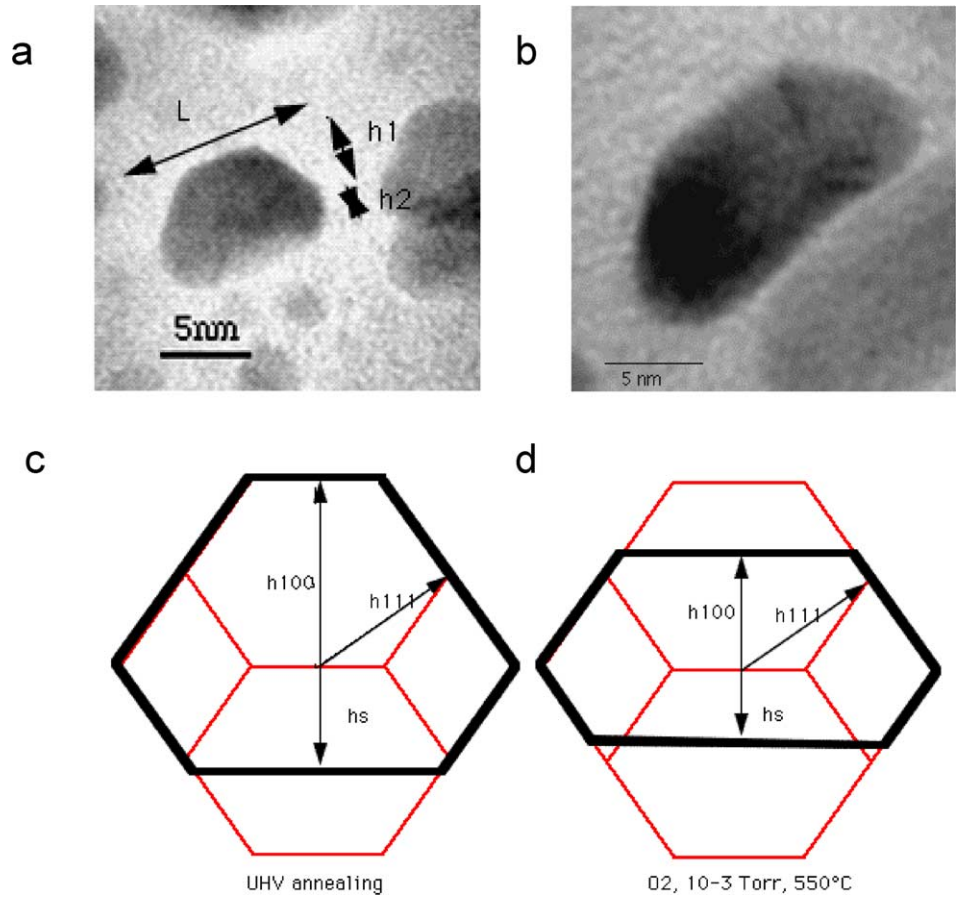

Fig. 5. Images of Pd crystallites on a MgO support annealed in UHV (a) and in 10^{-5} Torr of O_2 (b). There is a flattening of the particle and an increase in the (100) facet at the top versus the (111) facets, on the side. Profile view drawings of Pd particles annealed in UHV (c) or in O_2 (d) (10^{-3} Torr, 550 °C). The light drawings correspond to unsupported particles (reprinted from [37] with permission from Elsevier).

our research group permits imaging of metal particles in all of their orientations and aids in establishing particle shapes (as seen in Fig. 4). An alternative approach is the use of electron holography to obtain the amplitude and phase of the electron wave leaving the specimen. In this manner, we can reconstruct the depth of the sample along the electron beam and obtain 3D shapes in metal particles [34]. The work in our group showed how shapes of metal particles change after high-temperature treatment in reducing or oxidizing atmospheres. For example, in the case of Pt, reducing atmospheres caused the shapes to be cubooctahedral, whereas oxidizing atmospheres led to more spherical shapes [35].

The most definitive studies of shape changes of small crystals have been performed by researchers at Marseille [36,37], first using an SEM, and later with high-resolution TEM. By performing studies under UHV conditions, and carefully annealing the metal particles, it was possible to study the equilibrium shapes of metal particles. In case of metals such as Pd, it is very difficult to work under conditions where the bulk oxide PdO does not form. By annealing at low oxygen pressures [37], it was possible to preserve Pd in its metallic form. Fig. 5 shows the shapes of Pd particles annealed in UHV or in 10^{-5} Torr of O_2. The (100) facets grow at the expense of the (111) facets after annealing in oxygen atmospheres. These shape changes are consistent with the effect of adsorbed oxygen on surface energy of Pd, as predicted by the Wulff construction [37].

6. Surface structures of small particles (dynamic rearrangements)

Profile view images permit the most direct observation of the surfaces of small metal particles, as first reported by Marks and Smith [38]. As well as clean, sharp surface images, morphological details of catalytic significance, such as the distribution of surface steps, particle faceting, and the nature of surface reconstructions, were obtained. By matching the atom positions with calculations of particle structure, these authors were able to confirm the expected (1×2) reconstruction of the Au surface. A different technique, reflection electron microscopy, was developed by Cowley's group [39], where sample surfaces were oriented so that the diffracted beams could be used to form an image. In this geometry, the image is severely foreshortened, but unlike its complementary technique, reflection high-energy electron diffraction, they were able to obtain real space images of surface structure on metal and ceramic surfaces.

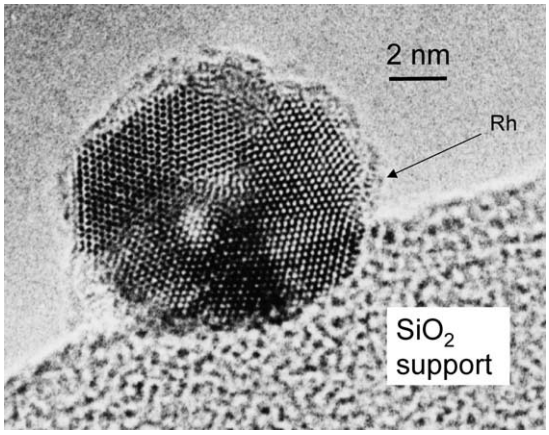

Fig. 6. HRTEM image of Rh/SiO_2 after oxidation–reduction cycling. The catalyst shows higher activity and altered selectivity due to the rougher exposed surfaces compared to the annealed state, shown in Fig. 4 (reprinted from [26] with permission from American Chemical Society).

It is well known from the work of Schmidt and coworkers [40] that oxidation and low-temperature reduction leads to large increases in the activity of metal catalysts for structure sensitive reactions. In our group, we studied the effect of oxidative restructuring on the surfaces of Rh metal particles [26]. Images of Rh metal surfaces in their annealed (high-temperature reduced) state were shown in Fig. 4. Fig. 6 shows an image of Rh particles in the oxidized and low-temperature reduced states, showing clearly how rough surfaces can be created on metal particles. These images show that the natures of surface sites in metal particles are not a function of size alone. In similarly sized particles, one can have very different surface coordinations leading to marked differences in activity. Further, it is commonly thought that oxidation will lead to spreading and wetting of the metal oxide on the support. However, we find that noble metals such as Pd or Rh form oxide particles that remain three-dimensional in shape [41]. A slight increase in size is caused by swelling of the particle due to a greater mass and the lower density of the oxide. It is the difference in specific volume of the metal and metal oxide phases that gives rise to this restructuring, leading to enhanced activity and altered selectivity.

Of great importance for the study of shape and surface structure changes in catalysts is the development of in situ TEM. With the advent of high-voltage microscopes, it becomes possible to achieve atomic resolution in the presence of a gas atmosphere. The first report of high-resolution observation in the presence of a gas phase was by Parkinson [42]. Later, Boyes et al. [43], modified a 300-keV TEM to enable operation in the presence of several Torr of gas allowing in situ studies of oxidation catalysts [44]. Most recently, the work at the Topsoe laboratories [45] has reported the use of in situ TEM to study changes in the catalytic surfaces after exposure to the gas phase. Fig. 7 shows shape changes in the Cu/ZnO catalyst that is used for methanol synthesis as a function of gas atmosphere. These shape changes, which lead to the flattening of the metal particles, allow these authors to explain the changes in reactivity seen when operating under more oxidizing conditions.

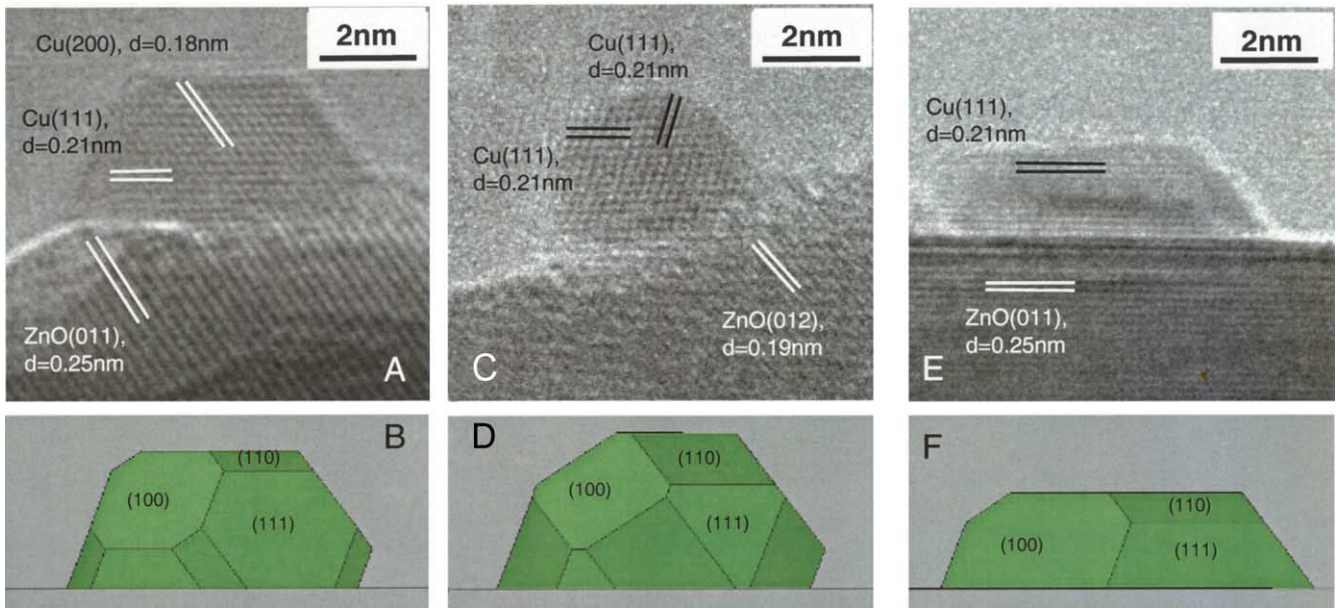

Fig. 7. In situ TEM images (A, C, and E) of a Cu/ZnO catalyst in various gas environments together with the corresponding Wulff constructions of the Cu nanocrystals (B, D, and F). (A) The image was recorded at a pressure of 1.5 mbar of H_2 at 220 °C. The electron beam is parallel to the [011] zone axis of copper. (C) Obtained in a gas mixture of H_2 and H_2O, H_2:H_2O = 3:1 at a total pressure of 1.5 mbar at 220 °C. (E) Obtained in a gas mixture of H_2 (95%) and CO (5%) at a total pressure of 5 mbar at 220 °C (reprinted from [45] with permission from American Association for the Advancement of Science).

7. Three-dimensional TEM

One major limitation of TEM imaging is that we obtain two-dimensional images from samples that are three-dimensional. Over the past decade, several approaches have emerged to fill in this information gap in the third dimension. It should be recognized first that image contrast cannot be directly interpreted in terms of sample thickness. As explained previously, when a metal particle appears dark, it simply means that it is oriented close to its diffraction condition. Image contrast is a complicated function of particle orientation, internal structure, and electron imaging conditions. Electron holography provides a method to obtain separately the phase and amplitude of the electron wave that exits a specimen. Phase shifts are directly related to mean inner potential, which in turn is related directly to the thickness of the sample. To obtain a hologram, one approach is off-axis holography, where a charged wire above the viewing screen serves as a biprism, and an interference pattern is generated between the electron wave that passes through the specimen and a reference wave going through vacuum. From this interference pattern (hologram), through Fourier processing, we can derive the phase and amplitude of the transmitted wave. These phase images provide direct thickness maps of the sample. Using this technique, we were able to map out the internal structure of Pd metal particles subjected to oxidation reduction treatments [46].

An alternative approach is that developed by the group of Krijn De Jong and coworkers [47,48], where a series of images are recorded from the sample as a function of tilt angle. By covering a large range of tilt angles, and combining these images, it is possible to create a 3D reconstruction of the sample. One can then obtain slices through the sample to investigate internal details of the particle. As shown in the image in Fig. 8, which represents slices through a grain of a zeolite particle, it is possible to image the location of mesopores within the particle. An extension of this approach by Weyland et al. [49] to small metal clusters in mesoporous silica has extended the resolution of this technique to nanoscale particles.

8. Scanning electron microscopy

A technique that shows great promise for the study of catalysts is scanning electron microscopy. Over the past decade, the resolution of commercially available SEMs in the low kilovolt range has been steadily improving. It is now possible to get probe sizes of about 25 Å at 1 keV and 5 Å at 30 keV [50]. The conventional operating mode for SEMs has been to operate at voltages of 25–30 keV, where the finest probe sizes can be obtained. Higher voltage operation is suitable for studying metal particles on conducting substrates such as carbon. On other supports, it is often necessary to provide a metallic coating to improve charge dissipation, but this step should be avoided whenever possible because features of interest are obscured. When the substrate is flat and yields little topographic contrast, it is possible to easily resolve and quantify nanosized metal particles using secondary electron imaging (SEI), but even better with back scattered electron imaging (BEI), which yields improved contrast. The SEM is most sensitive to metal particles on the surface of the support, but as shown by Liu [51], even particles located in the interior can be imaged using BEI imaging. Fig. 9 shows an example from the work of Liu [51] that shows how differences in operating voltage and imaging conditions (SEI or BEI) can alter the visibility of small Pt metal particles. For such samples, the SEM could easily supplant the TEM in the

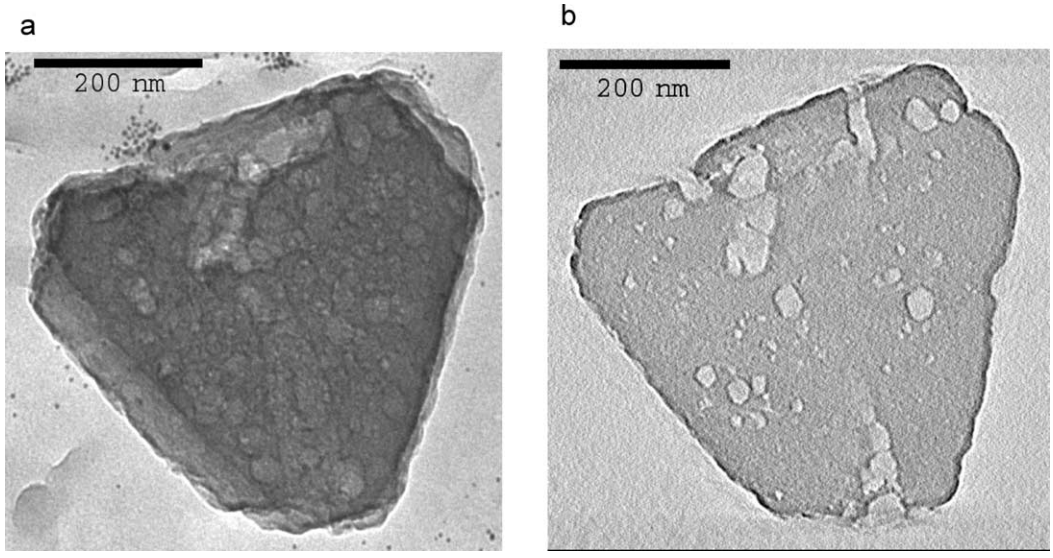

Fig. 8. TEM image of crystal of XVUSY zeolite. (a) 2D conventional TEM image and (b) slice through the particles using 3D TEM. The location and morphology of internal pores can be clearly seen (reprinted from [48] with permission from Wiley VCH).

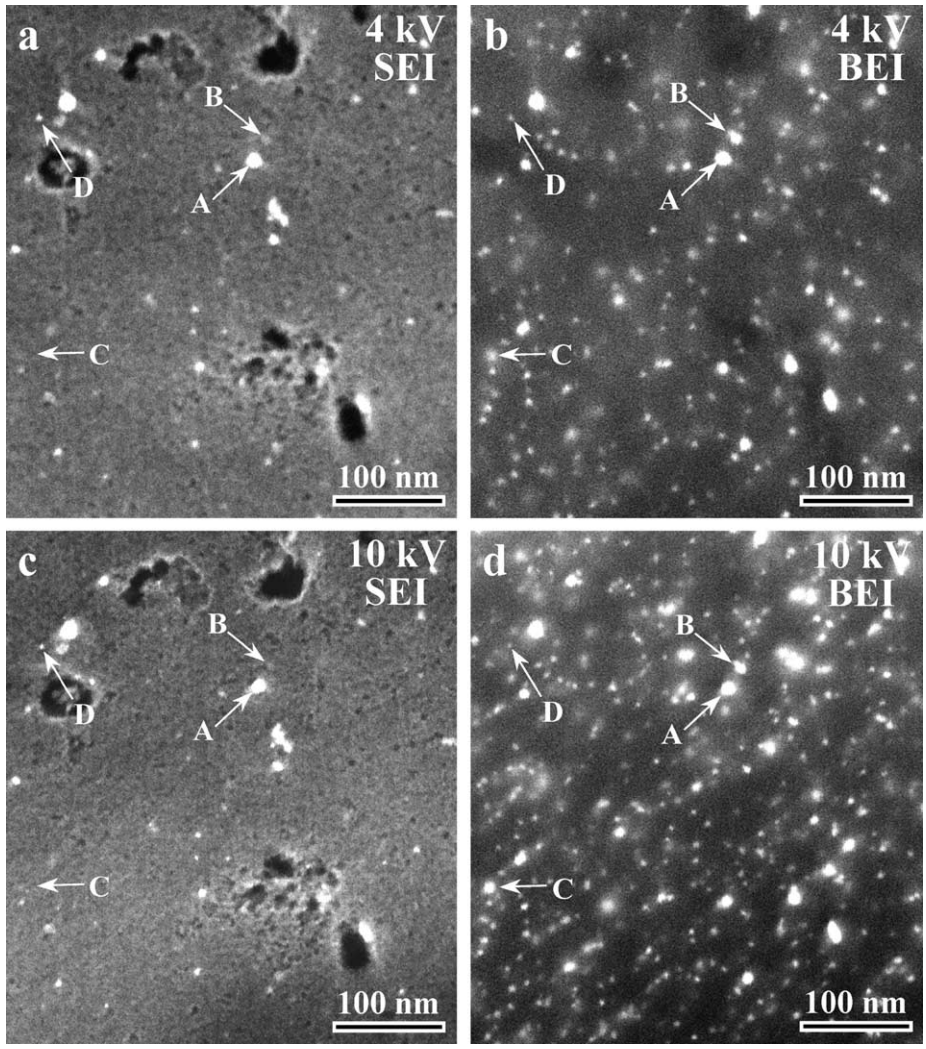

Fig. 9. High-resolution BE and SE images of the same sample area of a carbon-supported Pt catalyst at incident energies of (a), (b) 4 kV and (c), (d) 10 kV. A–D indicate Pt metal particles whose contrast varies with imaging conditions (reprinted from [51] with permission from Microscopy Society of America).

future as a routine characterization tool for studying metal dispersion and support morphology.

When more typical oxide (insulating) supports are used, and there is significant topographic contrast, identification of small metal particles becomes progressively more difficult. Here BE imaging is helpful since topographic contrast is suppressed relative to atomic number contrast. Use of lower operating voltages allows operation at the crossover point (where emission balances the influx of electrons) and the sample does not charge up. This is potentially the most useful area for application of the SEM for catalyst studies. Due to lower penetration of the electrons, the signal is derived from the surface region of the sample. Large areas of the sample can be imaged with minimal sample preparation. The larger probe size at lower operating voltages may preclude quantifying the observed nanoscale features, but the improved contrast and visibility may be very useful for understanding the morphological details of the catalyst sample. One example is presented from the work of Boyes [50]

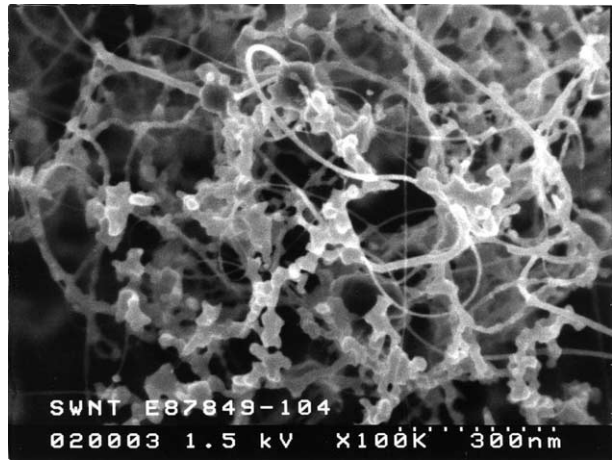

Fig. 10. Secondary electron image of processed single wall carbon nanotubes (SWNT) recorded at 1.5 kV. The smallest features correspond to single walled carbon nanotubes of widths less than 1 nm in diameter (reprinted from [50] with permission from Microscopy Society of America).

which shows the ability to detect nanosized features under low kilovolt (1.5 kV) operation in an SEM. The image in Fig. 10 shows single walled carbon nanotubes, with the associated catalyst particles, that provides a very good feel for the three-dimensional microstructure of this sample. While the dimension of individual nanotubes may be smaller than the probe width, their presence can be readily seen in SEM images.

9. In situ spectroscopy within the microscope (EDS, AES, EELS)

Electron beam specimen interactions cause inner shell excitations, which give rise to a number of signals: emission of photons, secondary and back scattered electrons, as well as Auger electrons. By using a small electron probe to excite the sample, direct information on elemental compositions can be obtained at the nanoscale. The most common application is the use of solid state X-ray detectors which perform energy dispersive spectroscopy of the generated photons. Recent developments in this technique are the availability of larger detectors (30 mm^2 compared to the most common 10 mm^2) and the ability to bring this detector closer to the specimen allowing an increase in the solid angle for X-ray collection. This makes it possible to acquire elemental compositions with very high spatial resolution. As illustrated in the work of Prestvik et al. [52], elemental analysis of nanometer-sized metal particles is now possible with considerable precision. The actual spatial resolution is still limited by the effects of beam broadening, but in thin regions of the sample, and with no overlap with neighboring particles, this may not be a serious issue.

Auger electrons, carrying chemical information, have also been used to form images of surface steps and small particles deposited on oxide substrates. Nanometer-resolution Auger electron images have been obtained in a specially modified UHV STEM instrument and small metal clusters containing as few as 15 atoms have been detected in Auger peak images by Liu and Cowley [53]. The combination of various imaging, diffraction, and analytical techniques has proved very powerful for characterizing surface structures with high spatial resolution and chemical sensitivity. However, the sensitivity for Auger electron detection is quite limited due to the limited space for a spectrometer in a TEM column. Combined with the necessity of having a UHV microscope, it has meant that this technique has not become widely available.

A technique that shows great promise is electron energy loss spectroscopy (EELS). Improvements in parallel detection of transmitted electrons and the availability of imaging EELS, allowing us to obtain energy filtered TEM images, makes this potentially a very useful technique for catalyst studies. The acquired spectra are complementary to EXAFS and provide similar information, but with high spatial resolution. Combined with the wider availability of field emission gun microscopes, both EELS and EFTEM will become increasingly important tools for the study of catalytic materials. An excellent review is presented by Colliex et al. [54]. An example of the type of information obtained can be seen in Fig. 11, where carbon K edge spectra are shown for some of the types of carbonaceous species seen in Fe Fischer–Tropsch catalysts [55]. These subtle differences in carbon structure lead to major differences in the reactivity of these different forms of carbon. XPS analysis of these same catalysts does not reveal the rich detail seen in these EELS patterns. Fig. 11 shows that the carbon in the iron

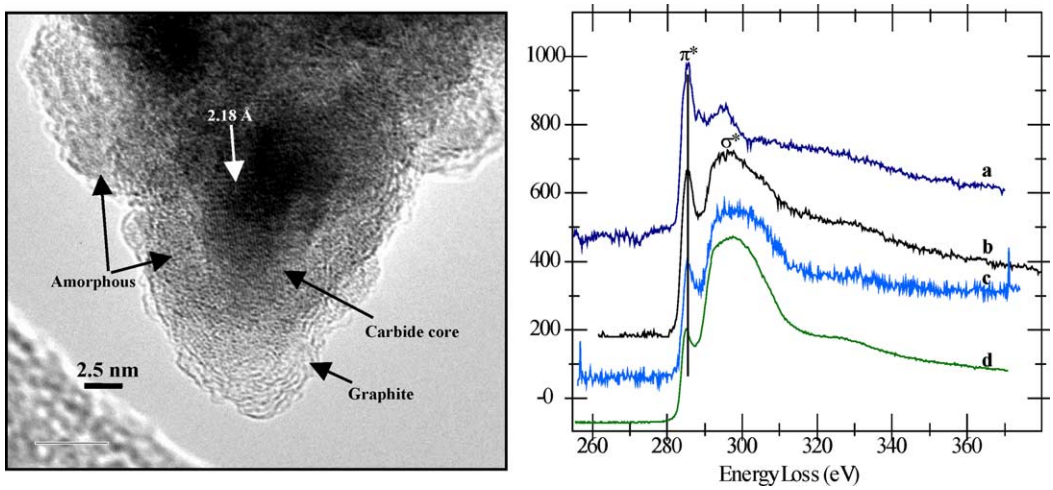

Fig. 11. HRTEM image of Fe catalyst (left) showing the carbide core, amorphous surface carbon layer, and some graphitic carbon. The EELS spectra on the right show the carbon K edge fine structure from different regions of a spent iron FT catalyst. (a) Carbide particle with an amorphous oxide layer (not seen in this image), (b) a carbide particle with an amorphous carbon layer (such as the one imaged here), (c) particle such as the one on the left after e-beam exposure, (d) reference C K edge recorded from the carbon film on the TEM grid, as seen in the bottom left corner of the image (reprinted from [55] with permission from Microscopy Society of South Africa).

carbide phase has a different ratio of the π^* and σ^* peaks compared to the amorphous surface carbon on the catalyst surface. We know from other results that the surface carbon is very reactive and can be converted to methane at low temperatures. Amorphous carbon films used to support these TEM samples are quite inert, but in TEM images you cannot distinguish them from these carbonaceous surface layers. The EELS spectra in Fig. 11 show that the surface carbonaceous layers are indeed different from the inert carbon films in their ratio of π^* and σ^* peaks. These results show that EELS in the TEM can be a very sensitive probe of reactivity and bonding of the nanoscale structures seen in catalysts.

10. Model catalysts

The nature of high-surface-area supports used to synthesize heterogeneous catalysts makes it inherently difficult to apply electron microscopy. The active phase is present within the pores, the supports are insulating and tend to charge up and become unstable during examination, and the contrast from the support interferes with images of the active phase. Hence, various forms of model catalysts have been used to simplify the study of catalysts. The most widely used model support for TEM studies consists of a thin oxide film that is supported on a TEM metal grid. The oxide film can be grown by evaporation of silicon or aluminum on a crystal of rock salt followed by oxidation of the metal and dissolution of the rock salt to yield a thin, self-supporting film that can be picked up on a TEM grid [40]. An interesting variation of this technique is the so-called "inverted" catalyst developed by the group of Hayek and coworkers [56]. Here the metal is first evaporated on rock salt and the oxide is next deposited, followed by dissolution of the rock salt so that the metal surface in contact with the rock salt is now exposed to the gas phase. In this manner, the metal surface in contact with the gas phase can be chosen based on the epitaxial relationship established during the evaporation of the metal on the substrate.

In our group, we have developed the use of nonporous metal oxides as supports, since they allow us to image the dispersed phase in edge-on as well as top view. These supports help to image the three-dimensional structure of the dispersed phase. The easiest ones to prepare are based on silica, as seen in Fig. 4, but crystalline, nonporous particles of transitional alumina can also be prepared using vapor phase routes [57]. It is worth mentioning that with the improvement in SEM image resolution, the requirement to prepare electron transparent support films can be relaxed. Thune et al. [58] have used silicon oxide layers grown on silicon wafers as model supports to study the polymerization of ethylene from single sites of a Cr polymerization catalyst. While silicon wafers may be adequate for some applications, they are not robust enough to be subjected to high temperatures. In our work on catalyst sintering, we have started to use disks of quartz or sapphire as model supports. These are excellent model supports that can be subjected to temperatures exceeding 1000 °C and provide very robust model catalysts for future microscopy studies using low-voltage SEM.

11. Future directions

This review has provided an account of some recent developments in microscopy of catalysts. We now discuss some of the improvements in microscopy techniques that could have a significant impact on the study of catalysts. The most important development on the horizon is the correction of aberrations in microscope lenses to improve resolution. While the development is underway for both scanning and transmission electron microscopes, of utmost importance would the application in scanning microscopes. Reducing the size of the probe below 1 Å in a STEM may make it possible to clearly see individual atomic and ionic species on the surface of catalyst supports. It is this missing "atomically dispersed" phase which is often invoked to explain the activity of supported catalysts. Another significant development is the improvement in resolution of low-voltage SEMs. With a low-voltage SEM, one could image a catalyst in its as-prepared state, without the need for metallic or carbon coating. We could map out the location of the active phase, on and below the surface of porous supports. The ability to directly image wash-coated monolith catalysts in the SEM and image nanoscale features would help immensely in diagnosing some of the causes of catalyst deactivation. Improvements in TEM resolution and low-dose techniques may allow us to study the internal structure of small metal clusters. At present, during high-magnification imaging, these metal clusters are quite mobile and details of internal structure get blurred. Future studies could be directed using low-dose techniques to better understand the nature of the metal-support interfaces. Finally, a development worthy of note is the availability of in situ microscopes that permit high resolution imaging in the presence of adsorbates and reactants. We have already seen application of these tools for studying the morphology of working catalysts. Improved resolution, lower beam dose, microscope stages that can correct for specimen drift will all contribute to the ease with which in situ microscopes could be used for the study of catalysts. With the application of in situ spectroscopic tools, better energy resolution to get EXAFS-like performance when performing EELS in the TEM, and the judicious use of model supports, we can extend significantly the impact of microscopy in the field of catalysis.

Acknowledgments

The author acknowledges financial support from the National Science Foundation (Grants CTS-99-11174 and CTS 98-71292) and the Department of Energy, Office

of Basic Energy Sciences (Grant DE-FG03-98ER14917). The author thanks the following for permission to include their previously published research in this review: Steve Pennycook, Bruce Gates, Larry Allard, Claude Henry, Poul Hansen, Krijn De Jong, Jimmy Liu, and Ed Boyes.

References

[1] A.K. Datye, D.J. Smith, Catal. Rev. Sci. Eng. 34 (1992) 129.
[2] M. Jose-Yacaman, G. Diaz, A. Gomez, Catal. Today 23 (1995) 161.
[3] A.K. Datye, in: G. Ertl, H. Knozinger, J. Weitkamp (Eds.), Catalyst Handbook, VCH, Weinheim/New York, 1997.
[4] J.M. Thomas, O. Terasaki, P.L. Gai, W.Z. Zhou, J. Gonzalez-Calbet, Acc. Chem. Res. 34 (2001) 583.
[5] J. Turkevich, J. Chem. Phys. 13 (1945) 235.
[6] Q. Xu, K.C.C. Kharas, A.K. Datye, Stud. Surf. Sci. Catal. 139 (2001) 157.
[7] S. Rossignol, C. Kappenstein, Int. J. Inorgan. Mater. 3 (2001) 51.
[8] P. Goodhew, Specimen Prep/Transmission Electron Microscopy of Materials, in: Royal Microscopical Society Microscopy Handbooks, Vol. 3, Springer, Berlin/New York, 1990.
[9] Y. Jin, A.K. Datye, in: Electron. Microsc. 1998, Proc. Int. Congr., 14th, Vol. 2, 1998, p. 379.
[10] J.O. Bovin, T. Huber, O. Balmes, J.O. Malm, G. Karlsson, Chem. Eur. J. 6 (2000) 129.
[11] S. Iijima, J. Appl. Phys. 42 (1971) 5891.
[12] D. Van Dyck, H. Lichte, K.D. van der Mast, Ultramicroscopy 64 (1996) 1.
[13] M.A. O'Keefe, C.J.D. Hetherington, Y.C. Wang, E.C. Nelson, J.H. Turner, C. Kisielowski, J.O. Malm, R. Mueller, J. Ringnalda, M. Pan, A. Thust, Ultramicroscopy 89 (2001) 215.
[14] G. Lang, H. Lichte, Eur. J. Cell Biol. 74 (1997) 67.
[15] A.V. Crewe, J.P. Wall, J.P. Langmore, Science 168 (1970) 1138.
[16] E.M. James, N.D. Browning, Ultramicroscopy 78 (1999) 125.
[17] S.J. Pennycook, B. Rafferty, P.D. Nellist, Microsc. Microanal. 6 (2000) 343.
[18] P.C. Flynn, S.E. Wanke, P.S. Turner, J. Catal. 33 (1974) 233.
[19] J. Schwank, L.F. Allard, M. Deeba, B.C. Gates, J. Catal. 84 (1983) 27.
[20] L.F. Allard, G.A. Panjabi, S.N. Salvi, B.C. Gates, Nano Lett. 2 (2002) 381.
[21] M.M.J. Treacy, S.B. Rice, J. Microscopy—Oxford 156 (1989) 211.
[22] S.B. Rice, J.Y. Koo, M.M. Disko, M.M.J. Treacy, Ultramicroscopy 34 (1990) 108.
[23] J.C. Yang, S. Bradley, J.M. Gibson, Microsc. Microanal. 6 (2000) 353.
[24] L.D. Marks, A. Howie, Nature 282 (1979) 196.
[25] D.J. Smith, L.D. Marks, Philos. Mag. A 44 (1981) 735.
[26] D. Kalakkad, S.L. Anderson, A.D. Logan, J. Pena, E.J. Braunschweig, C.H.F. Peden, A.K. Datye, J. Phys. Chem. 97 (1993) 1437.
[27] M.J. Yacaman, T. Ocanaz, Physica Status Solidi A Appl. Res. 42 (1977) 571.
[28] D.J. Smith, A.K. Petford-Long, L.R. Wallenberg, J.O. Bovin, Science 233 (1986) 872.
[29] R.T.K. Baker, E.B. Prestridge, R.L. Garten, J. Catal. 56 (1979) 390.
[30] A.D. Logan, E.J. Braunschweig, A.K. Datye, D.J. Smith, Langmuir 4 (1988) 827.
[31] D.J.C. Yates, L.L. Murrell, E.B. Prestridge, J. Catal. 57 (1979) 41.
[32] M.M.J. Treacy, A. Howie, J. Catal. 63 (1980) 265.
[33] A.K. Datye, N.J. Long, Ultramicroscopy 25 (1988) 203.
[34] A.K. Datye, D.S. Kalakkad, E. Voelkl, L.F. Allard, in: Electron Hologr., Proc. Int. Workshop, 1995, p. 199.
[35] A.S. Ramachandran, S.L. Anderson, A.K. Datye, Ultramicroscopy 51 (1993) 282.
[36] J.C. Heyraud, J.J. Metois, Acta Metall. 28 (1980) 1789.
[37] H. Graoui, S. Giorgio, C.R. Henry, Surf. Sci. 417 (1998) 350.
[38] L.D. Marks, D.J. Smith, Nature 303 (1983) 316.
[39] T. Hsu, J.M. Cowley, Ultramicroscopy 11 (1983) 239.
[40] S. Gao, L.D. Schmidt, J. Catal. 111 (1988) 210.
[41] A.K. Datye, J. Bravo, T.R. Nelson, P. Atanasova, M. Lyubovsky, L. Pfefferle, Appl. Catal. A 198 (2000) 179.
[42] G.M. Parkinson, Trans. R. Microsc. Soc. 1 (1990) 65.
[43] E.D. Boyes, P.L. Gai, L.G. Hanna, Mater. Res. Soc. Symp. Proc. 404 (1996) 53.
[44] P.L. Gai, Acta Crystallogr. Sect. B: Structur. Sci. B 53 (1997) 346.
[45] P.L. Hansen, J.B. Wagner, S. Helveg, J.R. Rostrup-Nielsen, B.S. Clausen, H. Topsoe, Science (Washington, DC) 295 (2002) 2053.
[46] L.F. Allard, E. Voelkl, D.S. Kalakkad, A.K. Datye, J. Mater. Sci. 29 (1994) 5612.
[47] A.J. Koster, U. Ziese, A.J. Verkleij, A.H. Janssen, K.P. deJong, J. Phys. Chem. B 104 (2000) 9368.
[48] A.H. Janssen, A.J. Koster, K.P. de Jong, Angewandte Chemie, Int. Ed. 40 (2001) 1102.
[49] M. Weyland, P.A. Midgley, J.M. Thomas, J. Phys. Chem. B 105 (2001) 7882.
[50] E.D. Boyes, Microsc. Microanal. 6 (2000) 307.
[51] J. Liu, Microsc. Microanal. 6 (2000) 388.
[52] R. Prestvik, B. Totdal, C.E. Lyman, A. Holmen, J. Catal. 176 (1998) 246.
[53] J. Liu, J.M. Cowley, Ultramicroscopy 48 (1993) 381.
[54] C. Colliex, M. Tence, E. Lefevre, C. Mory, H. Gu, D. Bouchet, C. Jeanguillaume, Mikrochim. Acta 114–115 (1994) 71.
[55] Y.M. Jin, H. Xu, A.K. Datye, in: Proc. 15th Int. Congr. Electron Microscopy, Vol. 1, 2002, p. 363.
[56] G. Rupprechter, K. Hayek, L. Rendon, M. Jose-Yacaman, Thin Solid Films 260 (1995) 148.
[57] S. Iijima, Surf. Sci. 156 (1985) 1003.
[58] P.C. Thune, J. Loos, A.M. De Jong, P.J. Lemstra, J.W. Niemantsverdriet, Top. Catal. 13 (2000) 67.